Electronic Supplementary Information (ESI)

Modulating *CO coverage via pyrrolic-N content on carbon for enhanced electrocatalytic CO_2 to CO

Fang Zhao, Yingzheng Zhang, Caiyue Wang, Jiatao Zhang, Di Zhao*

Key Laboratory of Cluster Science, Ministry of Education of China, Beijing Key Laboratory of Photoelectronic/Electrophotonic Conversion Materials, School of Chemistry and Chemical Engineering, Beijing Institute of Technology, Beijing 100081, China

Supporting Figure

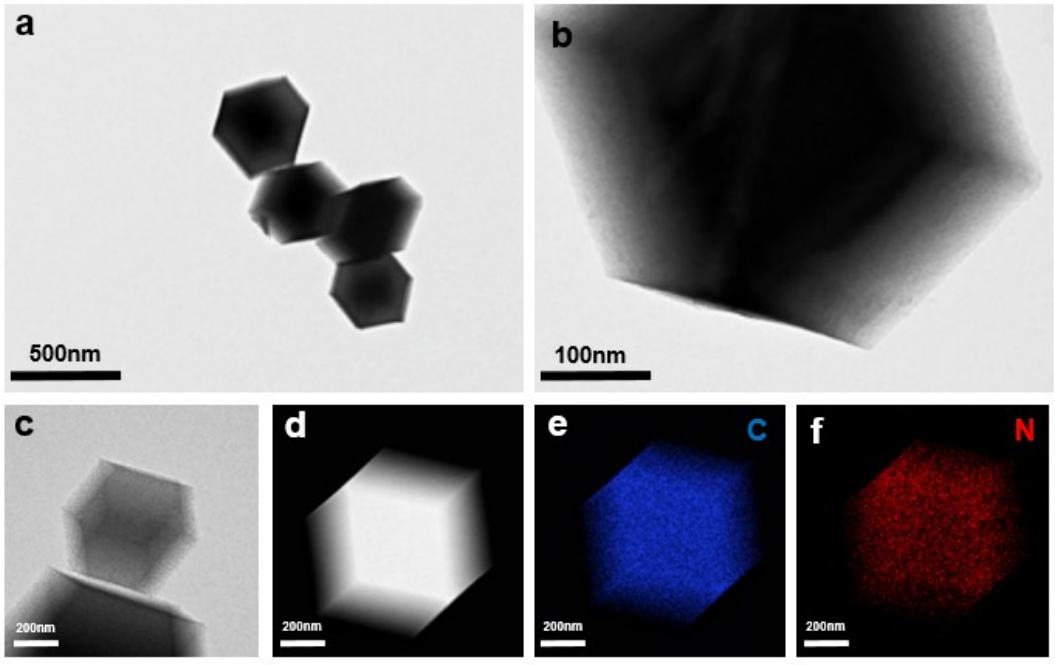

Figure S1. (a,b) Low- and (c) high-magnification TEM images of Pr-a-NC-H_2. (d-f) The EDS mapping of as-prepared Pr-a-NC-H_2 electrocatalyst.

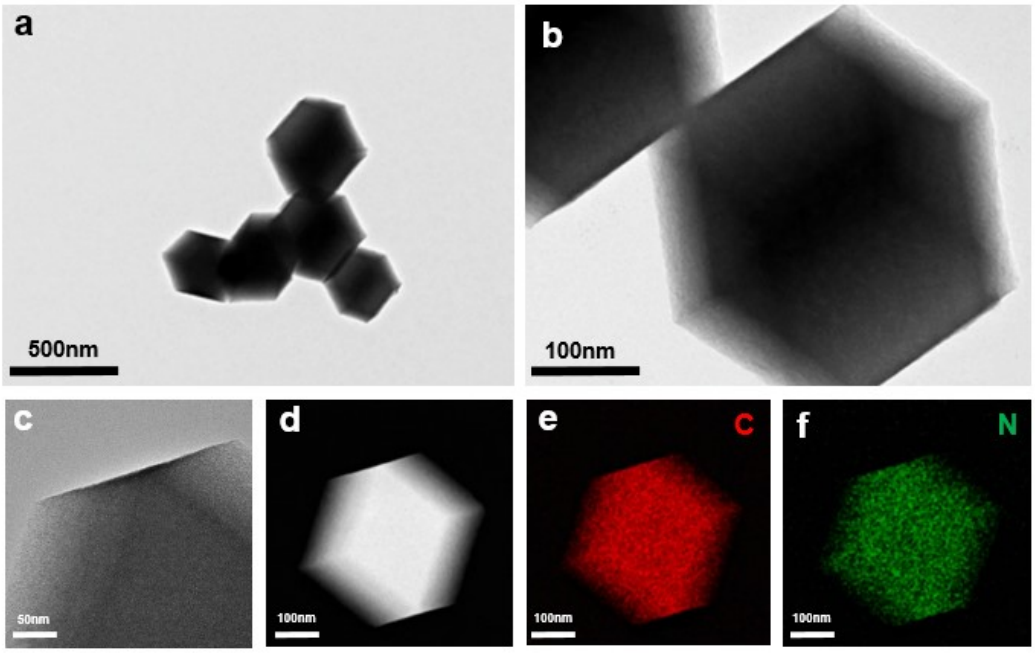

Figure S2. (a,b) Low- and (c) high-magnification TEM images of NC. (d-f) The EDS mapping of as-prepared NC electrocatalyst.

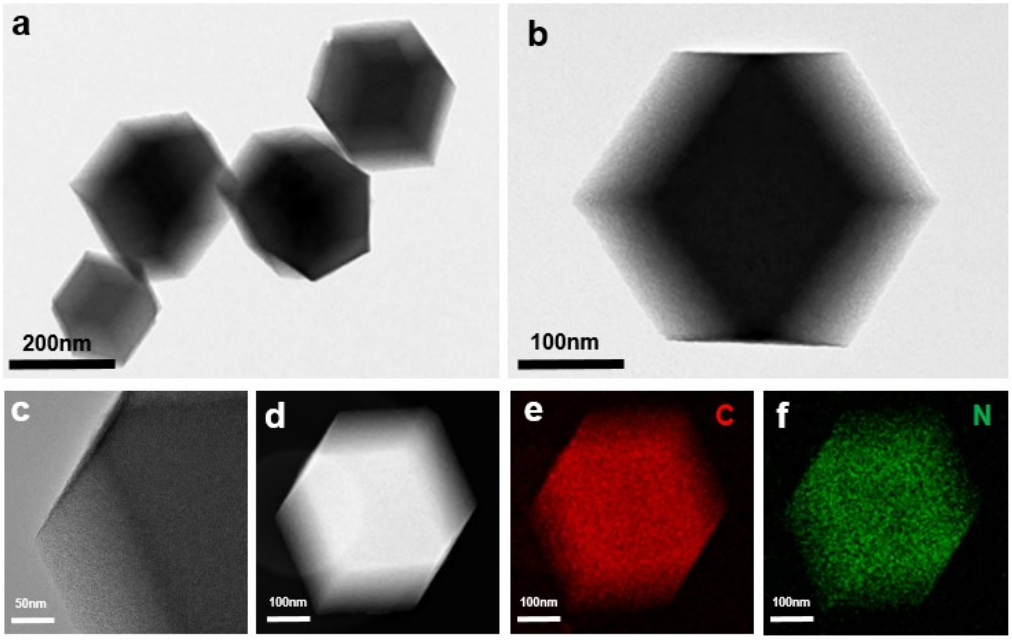

Figure S3. (a,b) Low- and (c) high-magnification TEM images of NC-H_2. (d-f) The EDS mapping of as-prepared NC-H_2 electrocatalyst.

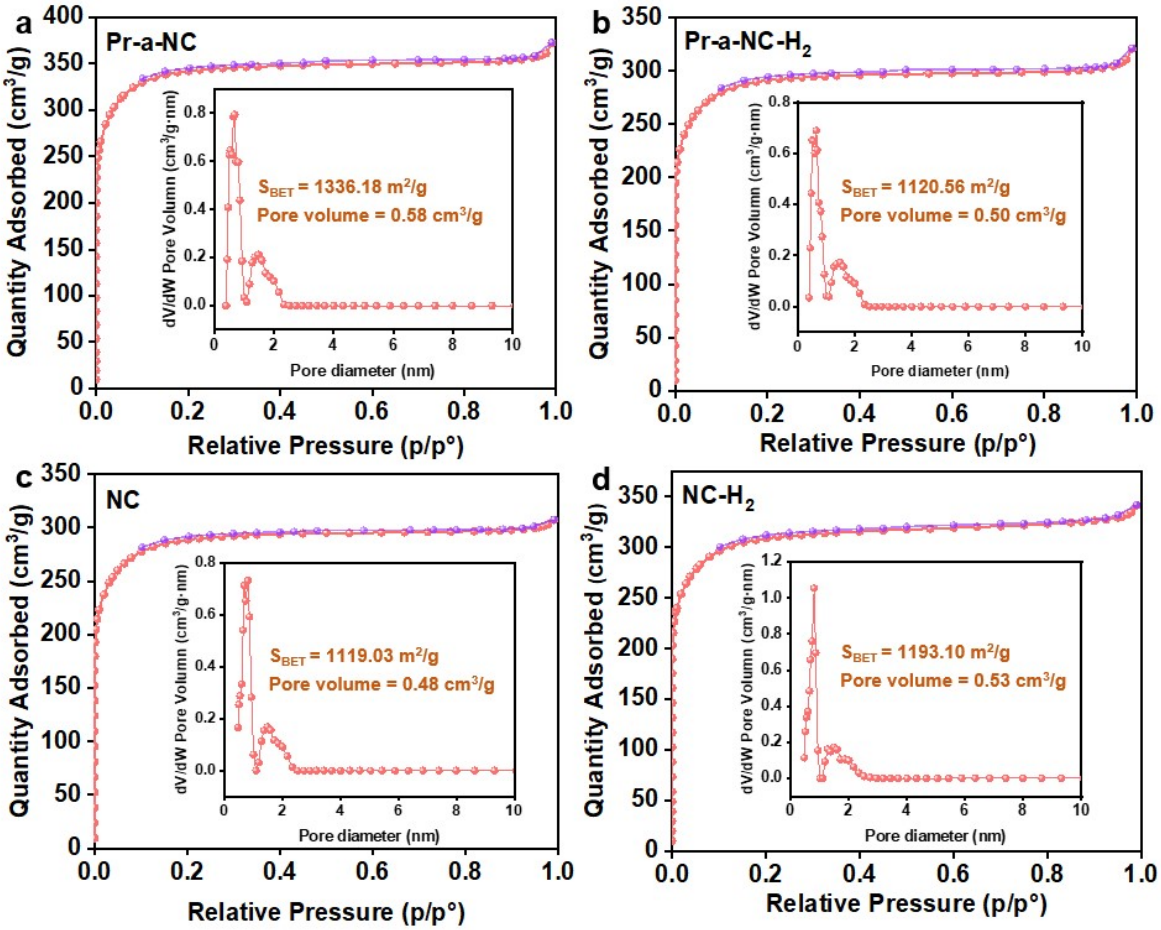

Figure S4. N_2 adsorption-desorption isotherms of (a) Pr-a-NC, (b) Pr-a-NC-H_2, (c) NC and (d) NC-H_2 electrocatalysts. Insets: Their corresponding pore size distribution curves.

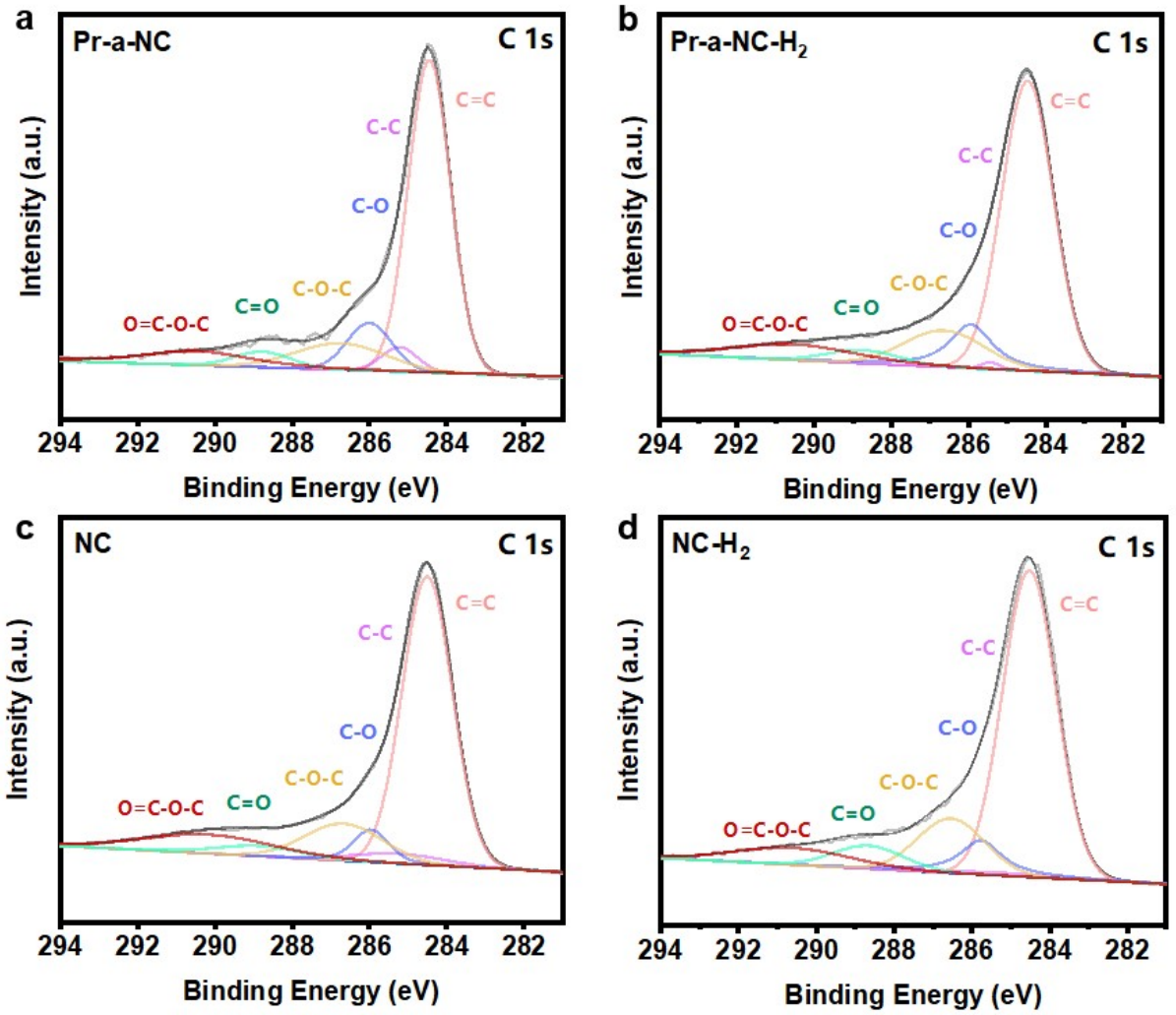

Figure S5. C 1s XPS spectra for (a) Pr-a-NC, (b) Pr-a-NC-H_2, (c) NC and (d) NC-H_2 electrocatalysts.

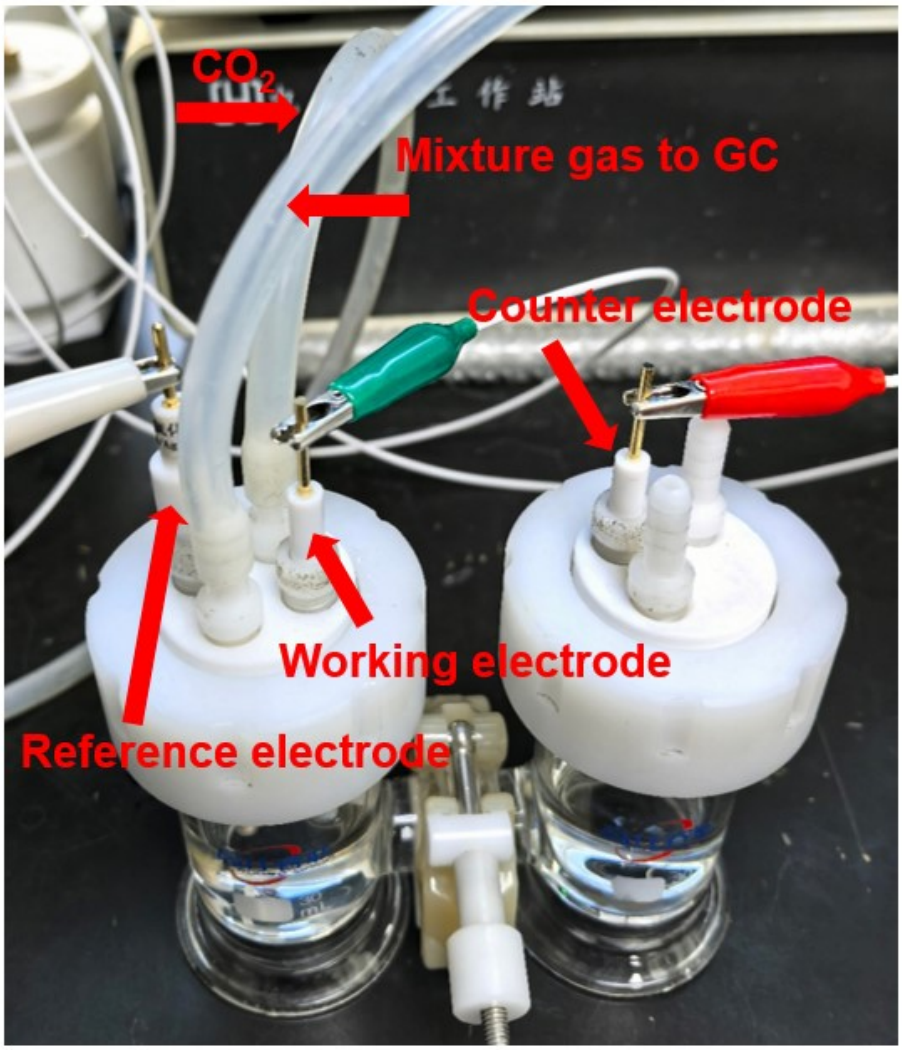

Figure S6. Digital photograph of an H-type cell for eCO_2RR.

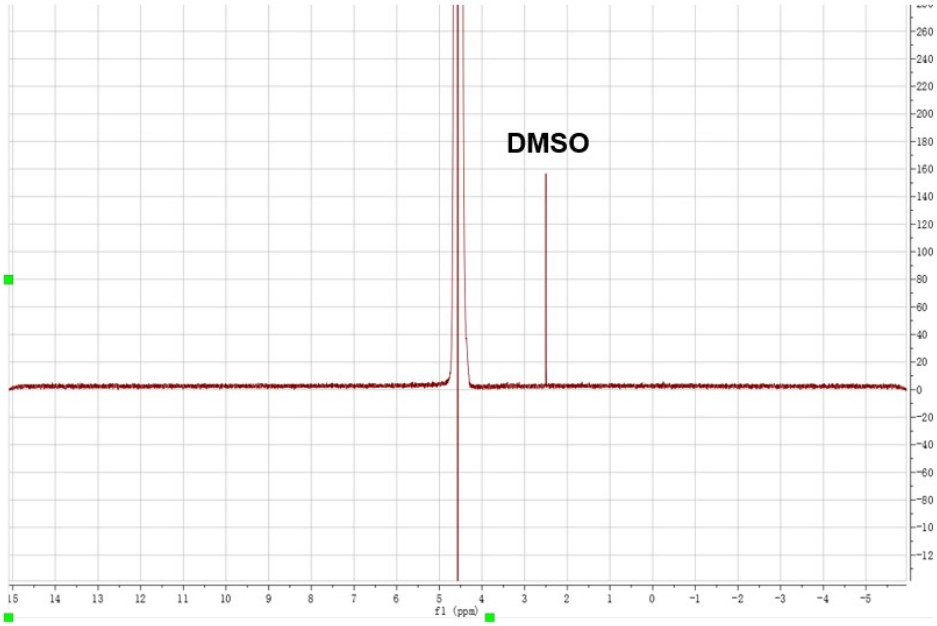

Figure S7. Characterization for the liquid product of Pr-a-NC at -0.6V vs RHE by ^{1}H nuclear magnetic resonance spectroscopy.

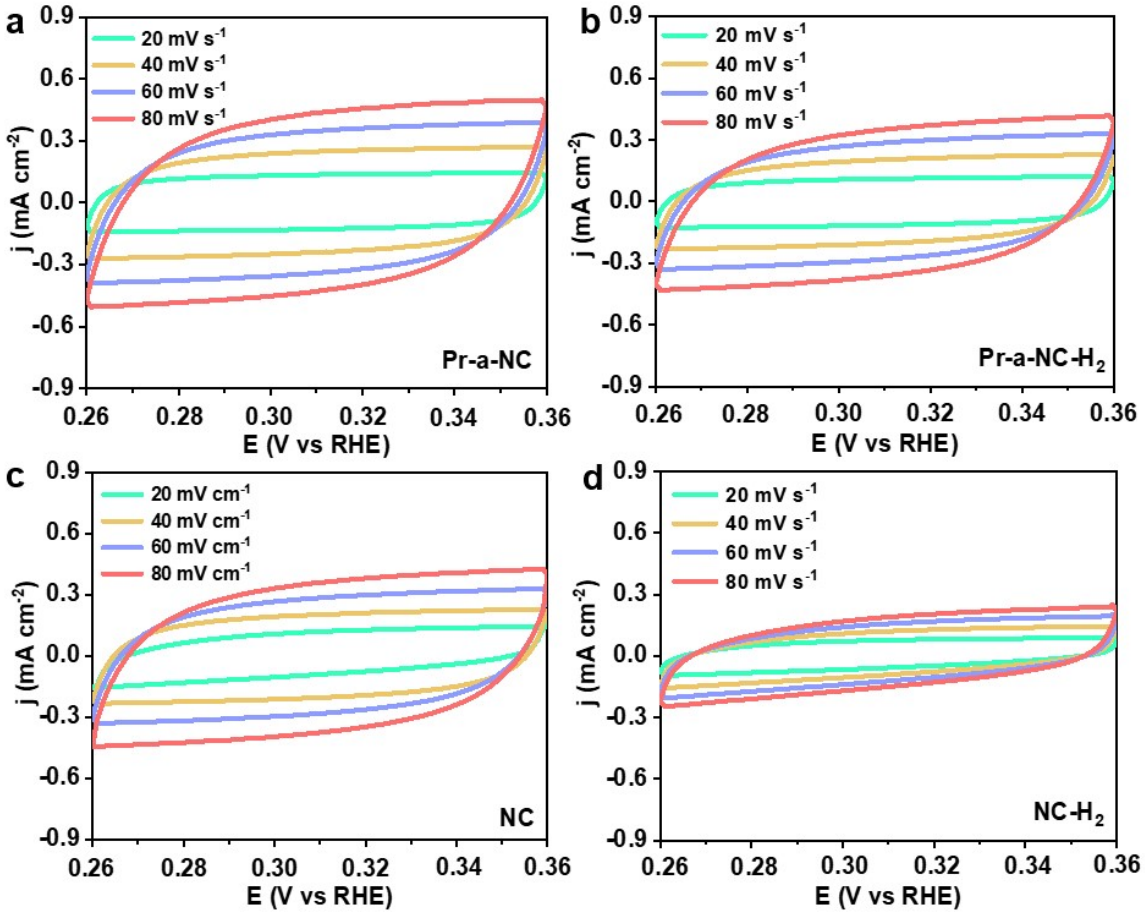

Figure S8. Cyclic voltammograms of (a) Pr-a-NC, (b) Pr-a-NC-H_2, (c) NC and (d) NC-H_2.

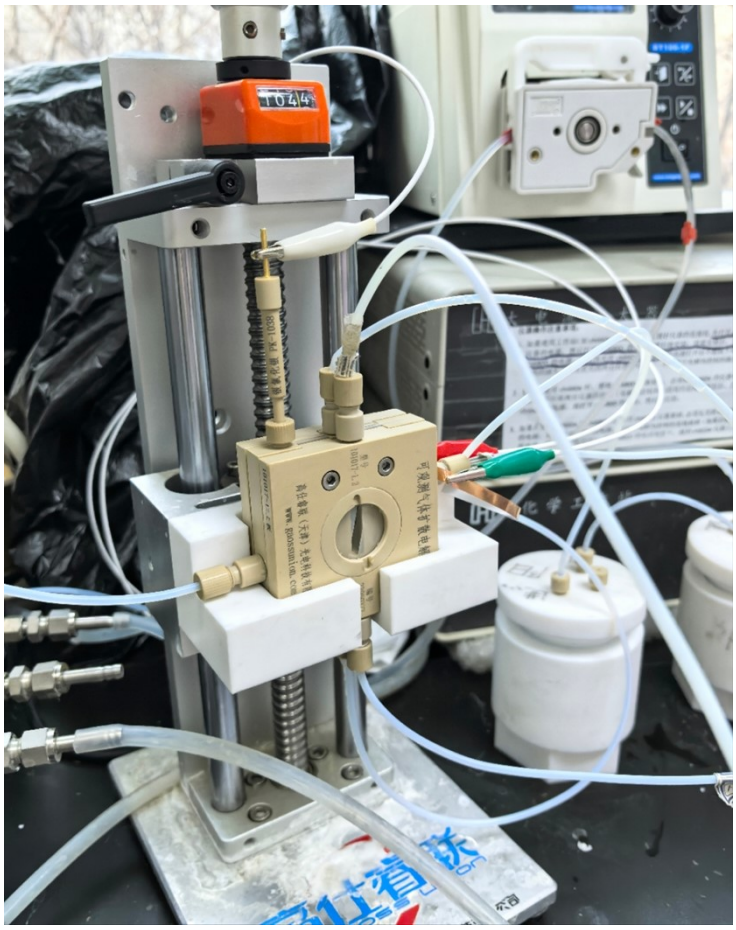

Figure S9. Digital photograph of the flow cell for eCO_2RR.

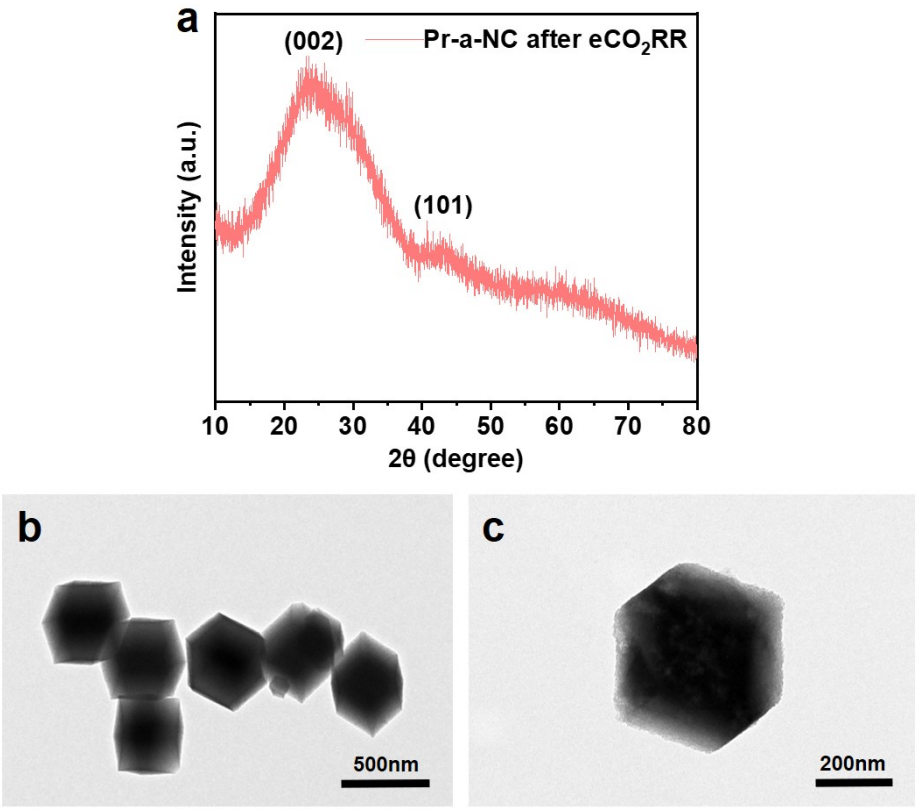

Figure S10. Structural characterization of Pr-a-NC electrocatalysts after eCO_2RR. (a) XRD pattern, (b-c) TEM images.

Table S1. Performance summary of four electrocatalysts.

Electrocatalyst	Relative pyrrolic-N content (%)	Current Density (mA cm^{-2})	FE_{CO} (%)
Pr-a-NC	44.00	31.73	92.08
NC	33.90	23.90	81.29
Pr-a-NC-H_2	28.11	23.35	79.53
NC-H_2	24.20	16.14	69.89